Published in final edited form as:
J Cereb Blood Flow Metab. 2009 February ; 29(2): 297–307. doi:10.1038/jcbfm.2008.119.

Gene profiles and electrophysiology of doublecortin-expressing cells in the subventricular zone after ischemic stroke

Xian Shuang Liu[1], **Michael Chopp**[1,2], **Xue Guo Zhang**[1], **Rui Lan Zhang**[1], **Ben Buller**[1,2], **Ann Hozeska-Solgot**[1], **Sara R Gregg**[1], and **Zheng Gang Zhang**[1]

[1]Department of Neurology, Henry Ford Hospital, Detroit, Michigan, USA

[2]Department of Physics, Oakland University, Rochester, Michigan, USA

Abstract

Stroke increases neuroblasts in the subventricular zone (SVZ) of the lateral ventricle and these neuroblasts migrate toward the ischemic boundary to replace damaged neurons. Using brain slices from the nonischemic adult rat and transgenic mice that expressed enhanced green fluorescent protein (EGFP) concomitantly with doublecortin (DCX), a marker for migrating neuroblasts, we recorded electrophysiological characteristics while simultaneously analyzing the gene expression in single SVZ cells. We found that SVZ cells expressing the DCX gene from the nonischemic rat had a mean resting membrane potential (RMP) of −30mV. DCX–EGFP-positive cells in the nonischemic SVZ of the transgenic mouse had a mean RMP of −25±7mV and did not exhibit Na^+ currents, characteristic of immature neurons. However, DCX–EGFP-positive cells in the ischemic SVZ exhibited a hyperpolarized mean RMP of −54±18 mV and displayed Na^+ currents, indicative of more mature neurons. Single-cell multiplex RT-PCR analysis revealed that DCX–EGFP-positive cells in the nonischemic SVZ of the transgenic mouse expressed high neural progenitor marker genes, Sox2 and nestin, but not mature neuronal marker genes. In contrast, DCX–EGFP-positive cells in the ischemic SVZ expressed tyrosine hydroxylase, a mature neuronal marker gene. Together, these data indicate that stroke changes gene profiles and the electrophysiology of migrating neuroblasts.

Keywords

electrophysiology; gene profiles; neural progenitor cells; neuroblasts; stroke; subventricular zone

Introduction

In the adult rodent brain, neurogenesis occurs primarily in the subventricular zone (SVZ) of the lateral ventricle and in the subgranular zone of the dentate gyrus (Gage *et al*, 1995; Luskin *et al*, 1997; Kirschenbaum *et al*, 1999; Alvarez-Buylla *et al*, 2000). The SVZ of adult rodent brain contains the migratory neuroblasts, actively proliferating progenitor cells and quiescent neural stem cells (Morshead *et al*, 1994; Garcia-Verdugo *et al*, 1998). Neuroblasts in the SVZ travel the rostral migratory stream to the olfactory bulb where they differentiate into granule and periglomerular neurons throughout adult life (Morshead *et al*, 1994; Garcia-Verdugo *et al*, 1998; Luskin, 1998). Migrating neuroblasts express doublecortin (DCX) and β-III tubulin (TuJ1). Using DCX-enhanced green fluorescent protein (DCX–EGFP) transgenic mice and immunostaining with antibodies against Tuj1 in wild-type mice, two groups have characterized

Correspondence: Dr ZG Zhang, Department of Neurology, Henry Ford Hospital, 2799 West Grand Boulevard, Detroit, MI 48202, USA., zhazh@neuro.hfh.edu.

biophysical properties and current profiles of migrating neuroblasts in acute brain slices (Bolteus and Bordey, 2004; Walker *et al*, 2007). DCX–EGFP cells in the SVZ and the dentate gyrus exhibit electrophysiological characteristics of immature and mature neurons, respectively, suggesting that DCX-expressing cells are a heterogeneous cell population (Walker *et al*, 2007).

Focal cerebral ischemia promotes neurogenesis in the SVZ and induces SVZ neuroblast migration toward the ischemic boundary (Parent *et al*, 2002; Zhang *et al*, 2001, 2004; Arvidsson *et al*, 2002; Jin *et al*, 2003). It is unknown whether ischemia affects electrophysiological properties of migrating neuroblasts. Moreover, gene profiles of migrating neuroblasts in the ischemic SVZ have not been investigated. Using single-cell multiplex RT-PCR combined with whole-cell patch-clamp recordings, we examined electrophysiological characteristics of SVZ neuroblasts in acute brain slices derived from DCX–EGFP transgenic mice subjected to middle cerebral artery occlusion (MCAo) and analyzed the simultaneous expression of 16 genes in a single DCX-expressing cell. We found that stroke changes gene profiles and electrophysiology of DCX-expressing cells in the SVZ.

Materials and methods

All experiments procedures were approved by the Institutional Animal Care and Use Committee of Henry Ford Hospital.

Animal Model of MCAo

A pair of breeding colony of DCX–EGFP transgenic mouse (DCX–GFP/bacterial artificial chromosome) was purchased from the Mutant Mouse Regional Resource Center. Adult DCX–EGFP animals (3 months) were identified by PCR analysis using tail DNA with primers to GFP (450 bp): forward 5′-TGCAGTGCTTCAGCCGCTACC-3′; reverse 5′-ATGTGATCGCGCTTCTCGTTG-3′. Male DCX–EGFP mice (3 months, $n = 14$) were subjected to the permanent focal cerebral ischemia by inserting a nylon filament (8 to 9mm in length) into the right MCA (Zhang *et al*, 1997). The mortality rate of this model in our hands is approximately 15% to 20%. All mice exhibited severe neurologic deficits 2 h after MCAo that persisted for 7 days. MCAo evokes a peak increase of neurogenesis 7 days after stroke (Zhang *et al*, 2001, 2004). Therefore, all mice were killed 7 days after MCAo. Nonischemic male Wistar rats (3 to 4 months, $n = 23$) were also used in this study.

Electrophysiology

Brain slices were prepared according to published protocols (Sakmann *et al*, 1989) that were modified. Briefly, rats or mice were anaesthetized with sodium pentobarbital (50 mg/kg body weight, intraperitoneally) and perfused with ice-cold artificial cerebral spinal fluid (ACSF) composed of the following (in mmol/L): 125 NaCl, 3 KCl, 2.5 $CaCl_2$, 1.5 $MgCl_2$, 25 $NaHCO_3$, and 10 Dextrose at pH 7.35 to 7.45 when equilibrated with 95% O_2 and 5% CO_2 for 3 mins. Brains were then quickly removed from the ice and placed in an oxygenated storage chamber containing ice-cold ACSF. Coronal slices containing the lateral ventricles (300 μm) were cut with a vibratome, incubated in oxygenated ACSF at 32°C for 30 mins and moved to room temperature (20 to 25°C). Thereafter, a coronal slice was mounted on a custom-made perfusion chamber, which was continuously perfused with oxygenated ACSF at 3.0 mL/mins and adjusted to a temperature of 37°C with HAAKE refrigerated circulator bath (Thermo Fisher Scientific Incorporation, Waltham, MA, USA). The brain slice was viewed under Nikon Eclipse E600-FN microscope (Nikon Corporation, Tokyo, Japan).

Whole-cell patch-clamp recordings were obtained as previously described (Sakmann *et al*, 1989). Patch pipettes were pulled from thin-walled borosilicate glass (World Precision

Instruments, Sarasota, FL, USA) on a PP-83 puller (Narishige, Tokyo, Japan). Pipettes had resistances of 8 to 10MΩ when filled with an intracellular solution containing the following (in mmol/L): 5.4 KCl, 132.6 K-gluconate, 0.3 $CaCl_2$, 1 EGTA, 10 HEPES, 1 $MgCl_2$, 2 mmol/L ATP, 0.25 GTP, and 4.6 neurobiotin. The pH and the osmolarity were adjusted to 7.35 (with KOH) and 290 mOsm, respectively. The liquid junction potential was corrected. Whole-cell recordings were performed using an AxoClamp 2B amplifier (Axon Instruments Incorporation, Foster City, CA, USA) and current signals were low-pass filtered at 2 to 5 kHz and digitized online at 5 to 20 kHz using a DigiDATA 1322A digitizing board (Axon Instruments Incorporation) and CyberAmp 320 programmable signal conditioner (Axon Instruments Incorporation) interfaced with a Dell computer (Round Rock, TX, USA). Settings were determined by compensating the transients of a small (5 mV) 10 ms voltage step. Capacitive and leak currents were not subtracted. Chemicals were obtained from Sigma-Aldrich (St Louis, MO, USA). Data acquisition, storage, and analysis were performed using PClampex 8.2 and Clampfit 8.2 (Axon Instruments Incorporation). Images of cells during patch-clamp recording were acquired via CCD camera (Nikon Corporation) and MetaVue software (Universal Imaging, Downingtown, PA, USA). All experiments were performed at room temperature (20 to 22°C).

Drug Applications

All drugs were bath applied by an eight-channel valve control system (ALA Scientific Instruments, New York, NY, USA). Chemicals were diluted in ACSF (pH 7.35). Sodium current inhibitor tetrodotoxin (TTX) and potassium current inhibitor tetraethyl ammonium (TEA) were successively bath applied for 2 mins before applying voltage step command. γ-Aminobutyric acid (GABA) blocker bicuculline and glutamate inhibitor 6-cyano-7-nitroquinoxaline-2, 3-dione (CNQX) were bath applied 10 secs before GABA and glutamate application.

Cytoplasm Harvest and Reverse Transcription

For single-cell RT-PCR experiments, the patch pipettes were filled with 6 μL of autoclaved internal RT-PCR solution containing: 140 mmol/L KCl, 5 mmol/L HEPES, 5 mmol/L EGTA, 3 mmol/L $MgCl_2$, pH 7.3. At the end of the recording (< 15 mins), the cell contents (including the nucleus in most cases) were aspirated as completely as possible into the patch pipette under visual control (× 40 objective) by application of gentle negative pressure. Cells were only analyzed further when the whole-cell configuration remained stable throughout the harvesting procedure. Pipettes were then quickly removed from the cell and washed twice through the solution interface. The pipette contents were expelled immediately into a 0.5 mL test tube. First-strand cDNA was synthesized for 5 mins at 65 °C in a total reaction volume of 13 μL, containing 1 μL oligo$(dT)_{20}$ primer, 1 μL 10 mmol/L dNTPs (Invitrogen Incorporation, Carlsbad, CA, USA), 4 μL 5× first-strand buffer, 1 μL of 0.1 mol/L DTT, 1 μL of RNaseOUT recombinant RNase inhibitor and 200U of reverse transcriptase (Superscript III; Invitrogen Incorporation). The reaction was further carried out at 50°C for 60 mins and then the reaction was inactivated by heating at 70° C for 15 mins. The single-cell cDNAs were kept at −80°C until PCR amplification.

Multiplex Single-Cell RT-PCR

Primer design and single-cell RT-PCR were performed based on methods previously described (Liss *et al*, 1999; Toledo-Rodriguez *et al*, 2004). In brief, primers were designed using OligoPerfect Designer software (Invitrogen Incorporation, Table 1). Possible interactions between primers were then tested. In addition, primers were subjected to a nucleotide database search to check for sequence specificity. To minimize exogenous contamination, all the solutions were autoclaved and bath solution was used as negative control for Multiplex PCR.

After reverse transcription, the cDNAs for different primers were mixed, and amplified first in a multiplex PCR with a subsequent single PCR using a Perkin-Elmer Thermal Cycler 480C (Applied Biosystem, Foster City, CA, USA). Multiplex-PCR was performed as hot start in a final volume of 30 μL containing 10 μL RT product, 0.1 μmol/L of each primer, and 15 μL Qiagen Multiplex mix (Qiagen, Valencia, CA, USA). The amplification consisted of 10 mins hot start at 95°C, followed by 28 cycles (40 secs at 94 °C, 40 secs at 56 °C, and 1 min at 72° C), followed by 10 mins at 72 °C. The single PCR amplifications were performed in a total volume of 20 μL containing 2 μL multiplex-PCR products, 0.2 mmol/L dNTPs, 1.5 mmol/L $MgCl_2$, 1μmol/L corresponding primer pair, and 1U Platinum Taq DNA polymerase. The single PCR amplification consisted of 12 individual reactions with 3 mins at 95 °C followed by 35 cycles (40 secs at 95 °C, 40 secs at 56°C, and 1 min at 72°C) and 10 mins at 72 °C. After amplification, the PCR products were analyzed on a 1.5% agarose gel.

Statistics

The data are presented as mean ± s.d. Independent sample *t*-test was used for two-group comparisons from the contralateral (nonischemic) and ipsilateral samples. Percentage data were analyzed using Pearson's χ^2-statistics. A value of $P < 0.05$ was taken as significant.

Results

Biophysical Properties and Gene Profiles of Nonischemic Svz Cells of the Adult Rat

The SVZ of the lateral ventricle in adult rodent contains a heterogeneous population of neural progenitor cells (Doetsch *et al*, 1997). Using whole-cell patch-clamp recordings, we recorded the rest membrane potential (RMP) in randomly selected SVZ cells of the nonischemic young adult rat (*n*=71 cells from *n* = 23 rats, Figure 1A). We observed two main types of RMP among these cells, one with a mean RMP of −75.1 ± 4.7 mV (*n* = 42 cells, Figure 1B) and the other with −30.5 ± 15 mV (*n* = 29 cells, Figure 1C). The mean RMP of ependymal cells determined by their cilia and location was −80.7 ± 2.2 mV (*n*=10 cells, Figure 1D).

To examine simultaneous gene profiles of a single cell characterized electrically, single-cell cytoplasm in the SVZ of the adult rat was captured by application of negative pressure to the patch-clamp pipette after recording the RMP. Using single-cell multiplex RT-PCR, we examined simultaneous expression of eight genes from a single SVZ cell: g0lial fibrillary acidic protein (GFAP, a marker of astrocytes), DCX (a marker of migrating neuroblasts), Sox2 (a marker of neural progenitor cells), glutamate receptor 5, glutamate decarboxylase isoform 65 (GAD65), solute carrier family 1 (glial high-affinity glutamate transporter 1, GLT-1), *N*-methyl-D-aspartate receptor 1, and β-actin as a house-keeping gene (Table 1). Using total RNA isolated from the brain tissue, the availability and specificity of primer sequences were verified before they were used in single-cell PCR. Cells (56%; 18 out of 32 cells) with a mean RMP of −73 mV expressed GFAP gene, and 10 out of 18 (56%) GFAP-expressing cells also expressed Sox2 gene (Figure 1E), suggesting that these are astrocytes and some of them could be neural stem cells (Figure 1E). All cells with a mean RMP of −30 mV (*n* = 19 cells) expressed DCX gene (Figure 1F). No cell expressed both DCX and GFAP. Among the DCX-expressing cells, 74%, 26%, and 31% of the cells also expressed Sox2 (14 out of 19 cells), GAD65 (5 out of 19 cells), and GLT-1 (6 out of 19 cells, Figure 1F and 1G), respectively. These transporter genes were detected in DCX + /Sox2 + or DCX + /Sox2– cells (Figure 1G), reflective of the heterogeneous cell property of neuroblasts in adult SVZ cells.

To examine the effect of glutamate and GABA on the membrane potential, we recorded the RMP after application of glutamate or GABA. Perfusion with glutamate induced a transient depolarization of GFAP-expressing SVZ cells in a dosage-dependent manner (Figure 2A and 2B), which was not blocked by an α-amino-3-hydroxy-5-methylisoxazole-4-propionic acid

receptor antagonist, CNQX (60 μmol/L, Figure 2C). Application of GABA (1 mmol/L, 20 secs) also induced a depolarization of GFAP-expressing cells, which was blocked by a competitive antagonist of GABA receptor, bicuculline (10 μmol/L, 20 secs, Figure 2D). This GABA response of GFAP-expressing cells is consistent with previous findings in GFAP-GFP transgenic mice (Liu *et al*, 2005, 2006). In contrast to GFAP-expressing cells, application of glutamate and GABA did not induce depolarization of the membrane in DCX-expressing neuroblasts (data not shown).

The Electrophysiology and Gene Profile of Ischemic DCX–EGFP Cells in the SVZ of the Adult Mouse

To examine the effects of stroke on electrophysiology of DCX-expressing cells, we used a DCX–EGFP transgenic mouse line. Under an epifluorescent microscope, living DCX–EGFP-positive cells in the SVZ of the lateral ventricle exhibited round cell bodies with one or two short process (Figure 3A). Using patch clamp, we patched a single DCX–EGFP-positive cell (Figure 3B and 3C) and then isolated the patched DCX–EGFP-positive cell (Figure 3D). The isolated single cell was processed for multiplex RT-PCR analysis. We found that DCX–EGFP-positive cells in the contralateral SVZ had a mean RMP of −25.1 ± 6.9 mV (n = 21 cells from 14 mice; Figure 3E, green diamond), which is comparable with rat data. These DCX–EGFP-positive cells did not respond to glutamate (n = 7 cells; Figure 3F) and GABA (n=6 cells; Figure 3F). However, DCX–EGFP-positive cells in the ipsilateral SVZ exhibited hyperpolarized mean RMP of −53.9 ± 17.7 mV (n = 30 cells from 14 mice; Figure 3E, red circle), which was significantly ($P < 0.001$) different from the RMP of the contralateral DCX–EGFP cells. The average activation time constant (τ) was significantly decreased in the ipsilateral DCX–EGFP-positive cells (Table 2). Other membrane properties, such as membrane capacitance (C_m) and access resistance (R_a) were not altered in these cells (Table 2). To activate outward and inward current, membrane potential was held at −80 mV and step voltage command pulses (−60 to + 45, 15 mV/step, 400 ms; Figure 4Aa) were applied. We detected Na^+ current in 3 of 10 DCX–EGFP-positive cells in the ipsilateral SVZ and the three cells exhibited a peak Na^+ current density of 15.7 ± 1.3 pA/pF (Figure 4Ab). Inhibition of K^+ current with TEA (10 mmol/L, 2 mins) blocked K^+ current but did not suppress the Na^+ current (Figure 4Ac, arrow). The Na^+ current was completely blocked by bath application of TTX (1 μmol/L, 2 mins; Figure 4Ad) and partially recovered 30 mins after withdrawing TTX (Figure 4Ae). However, the Na^+ current in these DCX–EGFP-positive cells was small compared with the Na^+ current detected in striatal neurons of nonischemic mice (142.8 ± 14.3 pA/pF, n = 3; Figure 4B). The Na^+ current was not detected in DCX–EGFP-positive cells in the contralateral SVZ (n = 10 cells, data not shown). In addition, DCX–EGFP cells in the ipsilateral SVZ showed a significant decrease of the amplitude of peak K^+ current (272 ± 109.0 pA, n = 10 cells, $P < 0.05$; Figure 4C and 4D) compared with DCX–EGFP-positive cells in the contralateral SVZ (381 ± 60.6 pA, n = 10 cells; Figure 4E and 4F). To dissect the components of K^+ current and to investigate their gating properties, TEA (10 mmol/L, 2 mins) was used by bath application. The peak K^+ current was reduced by ~60% in DCX–EGFP-positive cells after stroke (data not shown).

To examine whether eletrophysiological alterations of DCX–EGFP-positive cells are related to changes of gene profiles of these cells, 16 genes in a single DCX–EGFP-positive cell were analyzed (Table 1). In addition to seven genes used in the rat, DCX–EGFP-positive cells were screened for the expression of two neural progenitor marker genes, two sodium channel, and five interneuron marker genes (Figure 5). All DCX–EGFP-positive cells expressed the DCX gene (n = 26 cells from the ipsilateral SVZ and n = 21 cells from the contralateral SVZ, n = 14 mice), which confirms the specificity of this cell population. The majority of DCX cells expressing neural progenitor marker genes, Sox2, nestin, and Mash1 and stroke did not substantially alter gene patterns (Figure 5A–5E). DCX–EGFP cells (15% (3 out of 26 cells) and 38% (10 out of 26 cells)) in the ischemic SVZ expressed tyrosine hydroxylase (TH) and

calretinin (interneuron markers), respectively, whereas no DCX–EGFP cells (n = 21 cells) in the nonischemic SVZ expressed TH, and only 9% (2 out of 21 cells) of cells expressed calretinin (Figure 5A–5D). Interestingly, other calcium-binding protein genes, parvalbumin and calbindin, were not detected in any DCX–EGFP cells. Some DCX–EGFP-positive cells also expressed other genes including dopamine- and cAMP-regulated phosphoprotein with molecular weight of 32 kDa (DARPP32) and associated transporter Slc1a2. However, there was no substantial alteration of the gene expression between ischemic and nonischemic DCX–EGFP-positive cells (Figure 5E).

Discussion

The present study shows that DCX-expressing cells in the nonischemic SVZ of adult rodent expressed neural progenitor and interneuron marker genes, although these cells exhibited the same membrane electrical properties. Stroke changed the membrane electrical properties of DCX–EGFP cells in the ipsilateral SVZ of young adult mice to hyperpolarized mean RMP of −54 mV compared with depolarized mean RMP of −25 mV in the contralateral SVZ. In addition, stroke induced Na^+ currents of 110 pA in DCX–EGFP cells in the ipsilateral SVZ. Alteration of the membrane electrical properties in DCX–EGFP cells was associated with induction of TH and calretinin expression after stroke. These data indicate that stroke changes the gene profiles and electrophysiology of DCX-expressing cells in the SVZ.

In the SVZ of the young adult mouse, migrating neuroblasts identified by DCX- and TuJ1-positive cells comprise approximately 25% and 34% of total SVZ cell population, respectively (Bolteus and Bordey, 2004; Walker *et al*, 2007). The mean RMP of DCX- and TuJ1-positive cells in the SVZ of normal adult mouse is −25.4 ± 1.6 and −28.8 ± 0.4 mV, respectively (Bolteus and Bordey, 2004; Walker *et al*, 2007). Consistent with these published data, the current study shows that DCX–EGFP cells in the nonischemic SVZ had a mean RMP of −25.1 ± 6.9 mV. Using single-cell multiplex RT-PCR combined with whole-cell patch-clamp recordings, we found that DCX–EGFP-expressing cells in nonischemic SVZ had different profiles of gene expression, although DCX–EGFP-expressing cells exhibited a similar RMP. The majority of DCX–EGFP-expressing cells simultaneously expressed neural progenitor genes, Sox2, nestin, and Mash1, representing a population of early stage neuronal progenitor cells. Simultaneous expressions of DARPP32 and calretinin genes were detected in approximately 10% of DCX–EGFP-expressing cells. DARPP32 is expressed by striatal interneurons, whereas DCX-expressing cells in a postmitotic phase express calretinin (Brandt *et al*, 2003). Therefore, our data suggest that DCX–EGFP-expressing cells in the SVZ of adult rodent are a mixed population of neuroblasts, which is consistent with the previous findings (Walker *et al*, 2007).

The present study for the first time shows that stroke induced more hyperpolarized mean RMP (−54 mV) in DCX-expressing cells than that in nonischemic DCX-positive cells (−25 mV). Stroke also evoked peak Na^+ current amplitudes of 110 pA in 30% of DCX-expressing cells in young adult mice. The Na^+ current in DCX-expressing cells is specific because it was abolished by TTX but not by the K^+ current inhibitor TEA. Small amplitude Na^+ current without an action potential has been recorded in 60% of SVZ neural progenitor cells of postnatal mice (15- to 25-day-old; Wang *et al*, 2003). However, the present study did not detect the Na^+ current in nonischemic DCX-expressing cells of young adult transgenic mice (3-month-old), although all nonischemic DCX–EGFP-positive cells expressed sodium channel subunit genes. These data suggest that with age, DCX cells may lose the sodium current, although stroke induces DCX cells to recapture the current. Along with alterations of electrical properties, single-cell multiplex RT-PCR analysis revealed that stroke upregulated TH and calretinin expression in 15% and 38% of DCX-positive cells, respectively. TH is expressed by interneurons (Panzanelli *et al*, 2007; Benavides-Piccione and DeFelipe, 2007). In the dentate

gyrus where neuroblasts reside, the DCX-expressing cells develop into mature neurons (Walker *et al*, 2007). Therefore, we speculate that stroke may lead DCX-expressing cells in the SVZ to differentiate into relatively mature neurons. However, because of limited sample size, additional studies are warranted to investigate whether stroke leads DCX-expressing cells to commit to mature neuronal cells.

Neural progenitor cells in embryonic and adult mouse SVZ express K^+ channel genes, and blockage or activation of K^+ channel genes is associated with neural progenitor cell proliferation (Smith *et al*, 2008; Yasuda *et al*, 2008). During the acute stage of transient ischemia, the K^+ current is increased in CA1 pyramidal neurons of hippocampus, which has been implicated in causing neuronal death (Huang *et al*, 2001; Wei *et al*, 2003). Our results show that K^+ current was decreased in ischemic DCX–EGFP-positive cells. Although it remains to be determined whether changes in K^+ current affect proliferation of neuroblasts after stroke, the present study suggests that K^+ may be involved in ischemia-induced neurogenesis.

This study shows that GFAP but not DCX-expressing cells in the SVZ of young adult rodent (3-month-old) responded to glutamate and GABA stimulation. Using postnatal mice (15- to 25-day-old), others have shown that SVZ neural progenitor cells identified based on their morphology exhibited a depolarization in response to GABA (Wang *et al*, 2003; Stewart *et al*, 2002). A subpopulation of GFAP-expressing cells in the SVZ are neural stem cells that proliferate and differentiate into DCX-expressing cells (Doetsch *et al*, 1997; Merkle *et al*, 2004). Without geno- or phenotyping and electron microscopic characterization, it is challenging to distinguish different population of neural progenitor cells in the SVZ. Thus, the discrepancy between the present and published studies may reflect different cell populations that are measured.

In summary, our data show that stroke changed the membrane electrical properties of DCX-expressing cells in the SVZ of adult mice, which was associated with the expression of mature neuronal genes. This finding suggests that stroke may promote DCX-expressing neuroblast to become mature neurons.

Acknowledgments

This work was supported by NINDS grants PO1 NS23393, PO1 NS42345, and RO1HL 6476.

References

Alvarez-Buylla A, Herrera DG, Wichterle H. The subventricular zone: source of neuronal precursors for brain repair. Prog Brain Res 2000;127:1–11. [PubMed: 11142024]

Arvidsson A, Collin T, Kirik D, Kokaia Z, Lindvall O. Neuronal replacement from endogenous precursors in the adult brain after stroke. Nat Med 2002;8:963–970. [PubMed: 12161747]

Benavides-Piccione R, DeFelipe J. Distribution of neurons expressing tyrosine hydroxylase in the human cerebral cortex. J Anat 2007;211:212–222. [PubMed: 17593221]

Bolteus AJ, Bordey A. GABA release and uptake regulate neuronal precursor migration in the postnatal subventricular zone. J Neurosci 2004;24:7623–7631. [PubMed: 15342728]

Brandt MD, Jessberger S, Steiner B, Kronenberg G, Reuter K, Bick-Sander A, von der Behrens W, Kempermann G. Transient calretinin expression defines early postmitotic step of neuronal differentiation in adult hippocampal neurogenesis of mice. Mol Cell Neurosci 2003;24:603–613. [PubMed: 14664811]

Doetsch F, Garcia-Verdugo JM, Alvarez-Buylla A. Cellular composition and three-dimensional organization of the subventricular germinal zone in the adult mammalian brain. J Neurosci 1997;17:5046–5061. [PubMed: 9185542]

Gage FH, Ray J, Fisher LJ. Isolation, characterization, and use of stem cells from the CNS. Annu Rev Neurosci 1995;18:159–192. [PubMed: 7605059]

Garcia-Verdugo JM, Doetsch F, Wichterle H, Lim DA, Alvarez-Buylla A. Architecture and cell types of the adult subventricular zone: in search of the stem cells. J Neurobiol 1998;36:234–248. [PubMed: 9712307]

Huang H, Gao TM, Gong L, Zhuang Z, Li X. Potassium channel blocker TEA prevents CA1 hippocampal injury following transient forebrain ischemia in adult rats. Neurosci Lett 2001;305:83–86. [PubMed: 11376889]

Jin K, Sun Y, Xie L, Peel A, Mao XO, Batteur S, Greenberg DA. Directed migration of neuronal precursors into the ischemic cerebral cortex and striatum. Mol Cell Neurosci 2003;24:171–189. [PubMed: 14550778]

Kirschenbaum B, Doetsch F, Lois C, Alvarez-Buylla A. Adult subventricular zone neuronal precursors continue to proliferate and migrate in the absence of the olfactory bulb. J Neurosci 1999;19:2171–2180. [PubMed: 10066270]

Liss B, Bruns R, Roeper J. Alternative sulfonylurea receptor expression defines metabolic sensitivity of K-ATP channels in dopaminergic midbrain neurons. EMBO J 1999;18:833–846. [PubMed: 10022826]

Liu X, Bolteus AJ, Balkin DM, Henschel O, Bordey A. GFAP-expressing cells in the postnatal subventricular zone display a unique glial phenotype intermediate between radial glia and astrocytes. Glia 2006;54:394–410. [PubMed: 16886203]

Liu X, Wang Q, Haydar TF, Bordey A. Nonsynaptic GABA signaling in postnatal subventricular zone controls proliferation of GFAP-expressing progenitors. Nat Neurosci 2005;8:1179–1187. [PubMed: 16116450]

Luskin MB. Neuroblasts of the postnatal mammalian forebrain: their phenotype and fate. J Neurobiol 1998;36:221–233. [PubMed: 9712306]

Luskin MB, Zigova T, Soteres BJ, Stewart RR. Neuronal progenitor cells derived from the anterior subventricular zone of the neonatal rat forebrain continue to proliferate *in vitro* and express a neuronal phenotype. Mol Cell Neurosci 1997;8:351–366. [PubMed: 9073397]

Merkle FT, Tramontin AD, García-Verdugo JM, Alvarez-Buylla A. Radial glia give rise to adult neural stem cells in the subventricular zone. PNAS 2004;101:17528–17532. [PubMed: 15574494]

Morshead CM, Reynolds BA, Craig CG, McBurney MW, Staines WA, Morassutti D, Weiss S, van der Kooy D. Neural stem cells in the adult mammalian forebrain: a relatively quiescent subpopulation of subependymal cells. Neuron 1994;13:1071–1082. [PubMed: 7946346]

Panzanelli P, Fritschy JM, Yanagawa Y, Obata K, Sassoè-Pognetto M. GAB Aergic phenotype of periglomerular cells in the rodent olfactory bulb. J Comp Neurol 2007;20(502):990–1002. [PubMed: 17444497]

Parent JM, Vexler ZS, Gong C, Derugin N, Ferriero DM. Rat forebrain neurogenesis and striatal neuron replacement after focal stroke. Ann Neurol 2002;52:802–813. [PubMed: 12447935]

Sakmann B, Edwards F, Konnerth A, Takahashi T. Patch clamp techniques used for studying synaptic transmission in slices of mammalian brain. Q J Exp Physiol 1989;414:600–612.

Smith DO, Rosenheimer JL, Kalil RE. Delayed rectifier and a-type potassium channels associated with kv 2.1 and kv 4.3 expression in embryonic rat neural progenitor cells. PLoS ONE 2008;3:e1604. [PubMed: 18270591]

Stewart RR, Hoge GJ, Zigova T, Luskin MB. Neural progenitor cells of the neonatal rat anterior subventricular zone express functional GABA(A) receptors. J Neurobiol 2002;50:305–322. [PubMed: 11891665]

Toledo-Rodriguez M, Blumenfeld B, Wu C, Luo J, Attali B, Goodman P, Markram H. Correlation maps allow neuronal electrical properties to be predicted from single-cell gene expression profiles in rat neocortex. Cereb Cortex 2004;14:1310–1327. [PubMed: 15192011]

Walker TL, Yasuda T, Adams DJ, Bartlett PF. The doublecortin-expressing population in the developing and adult brain contains multipotential precursors in addition to neuronal-lineage cells. J Neurosci 2007;27:3734–3742. [PubMed: 17409237]

Wang DD, Krueger DD, Bordey A. GABA depolarizes neuronal progenitors of the postnatal subventricular zone via GABAA receptor activation. J Physiol 2003;550(Part 3):785–800. [PubMed: 12807990]

Wei L, Yu SP, Gottron F, Snider BJ, Zipfel GJ, Choi DW. Potassium channel blockers attenuate hypoxia- and ischemia-induced neuronal death *in vitro* and *in vivo*. Stroke 2003;34:1281–1286. [PubMed: 12677023]

Yasuda T, Bartlett PF, Adams DJ. K(ir) and K(v) channels regulate electrical properties and proliferation of adult neural precursor cells. Mol Cellr Neurosci 2008;37:284–297.

Zhang R, Zhang Z, Wang L, Wang Y, Gousev A, Zhang L, Ho KL, Morshead C, Chopp M. Activated neural stem cells contribute to stroke-induced neurogenesis and neuroblast migration toward the infarct boundary in adult rats. J Cereb Blood Flow Metab 2004;24:441–448. [PubMed: 15087713]

Zhang RL, Chopp M, Zhang ZG, Jiang Q, Ewing JR. A rat model of focal embolic cerebral ischemia. Brain Res 1997;766:83–92. [PubMed: 9359590]

Zhang RL, Zhang ZG, Zhan L, Chopp M. Proliferation and differentiation of progenitor cells in the cortex and the subventricular zone in the adult rat after focal cerebral ischemia. Neuroscience 2001;105:33–41. [PubMed: 11483298]

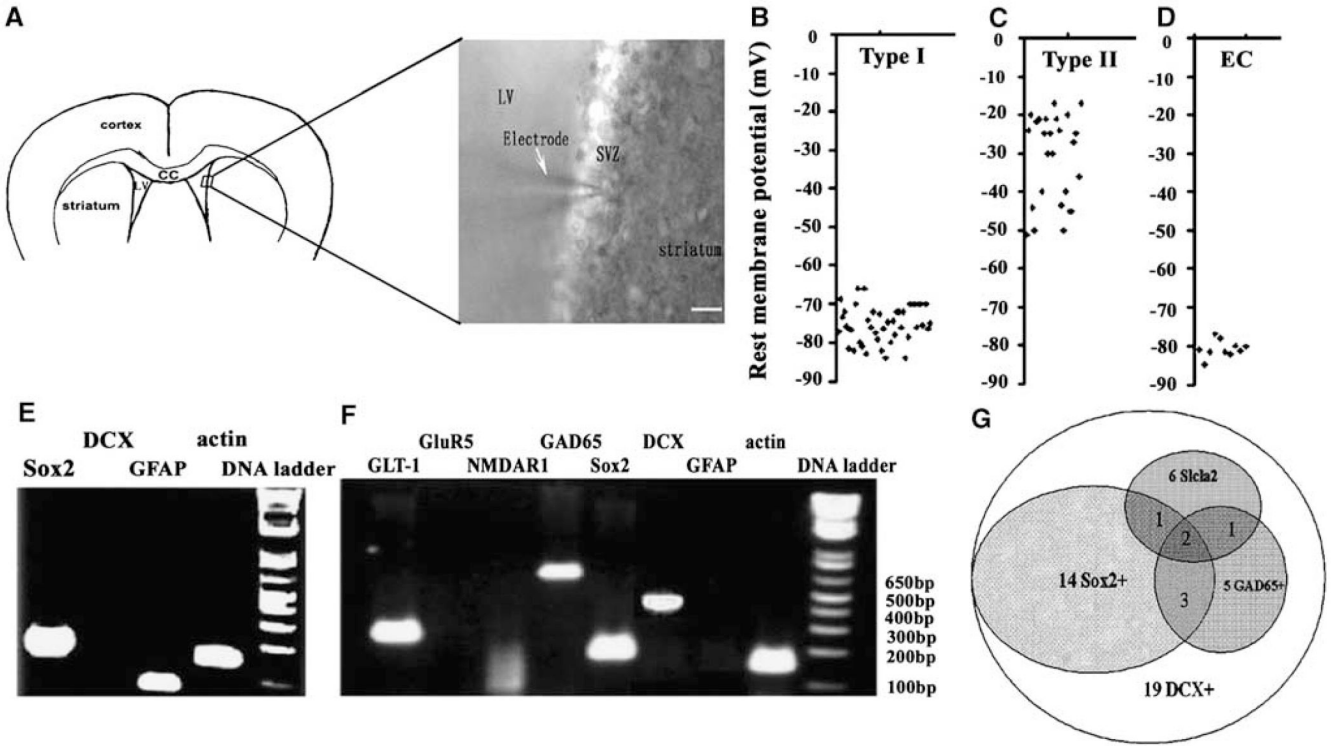

Figure 1.

Gene profiles of a single SVZ cell of nonischemic rat. A microphotograph shows a patch pipette approaching a SVZ cell of the lateral ventricle in a coronal brain slice (**A**). Scatter plots show types I (**B**, *n*=42) and II (**C**, *n*=29) rest membrane potential of individual SVZ cells and ependymal cells (**D**, *n*=10) of nonischemic rats. (**E–G**) Single SVZ cell RT-PCR products showing a single cell that simultaneously expresses GFAP and Sox2 genes (**E**) or DCX, Sox2, GAD65, and GLT-1 genes (**F**). Venn diagram (**G**) illustrates the coexpression number of Sox2, GAD65, and GLT-1 in single DCX-positive cells (*n*=19 cells). EC in (**D**) indicates ependymal cells. Bar in (**A**)=20 μm.

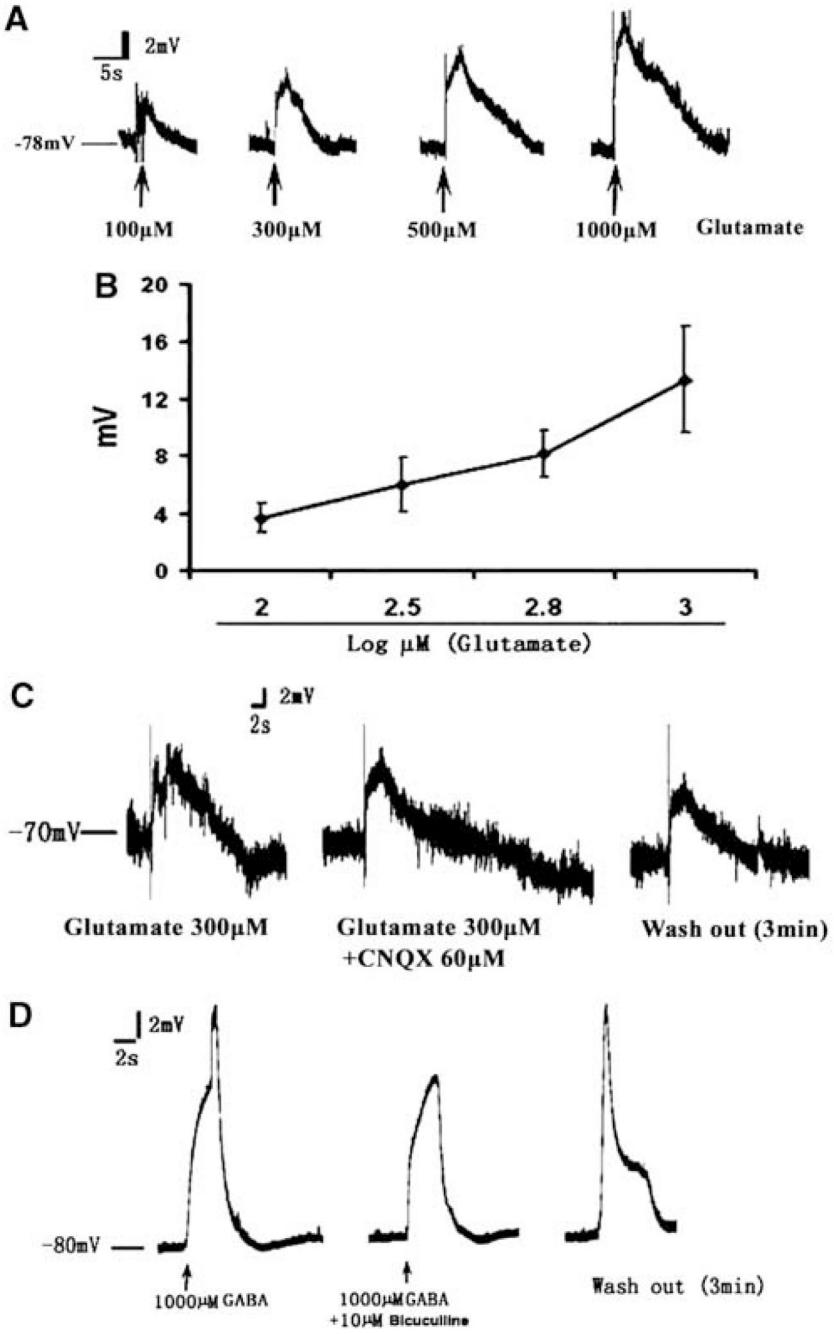

Figure 2.

The effect of glutamate and GABA on GFAP-expressing cells in the SVZ of the nonischemic rat. (**A**) A glutamate dose–response curve showing representative examples of potential alteration induced by rapid bath applications of glutamate at 100, 300, 500, and 1000 μmol/L (20 secs) onto the patched GFAP-positive cells. A fit to a sigmoidal logistic equation gives glutamate dose dependence (**B**, *n* = 4 to 6 per group). The presence of an AMPA receptor antagonist CNQX (**C**, glutamate 300 μmol/L + CNQX 60 μmol/L, 20 secs, *n* = 3) or washing out CNQX (**C**, wash out 3 mins) did not alter depolarization induced by glutamate (**C**, glutamate 300 μmol/L, 10 secs). However, GABA-induced depolarization was inhibited by its antagonist bicuculline (10 μmol/L, 20 secs, **D**, *n* = 3).

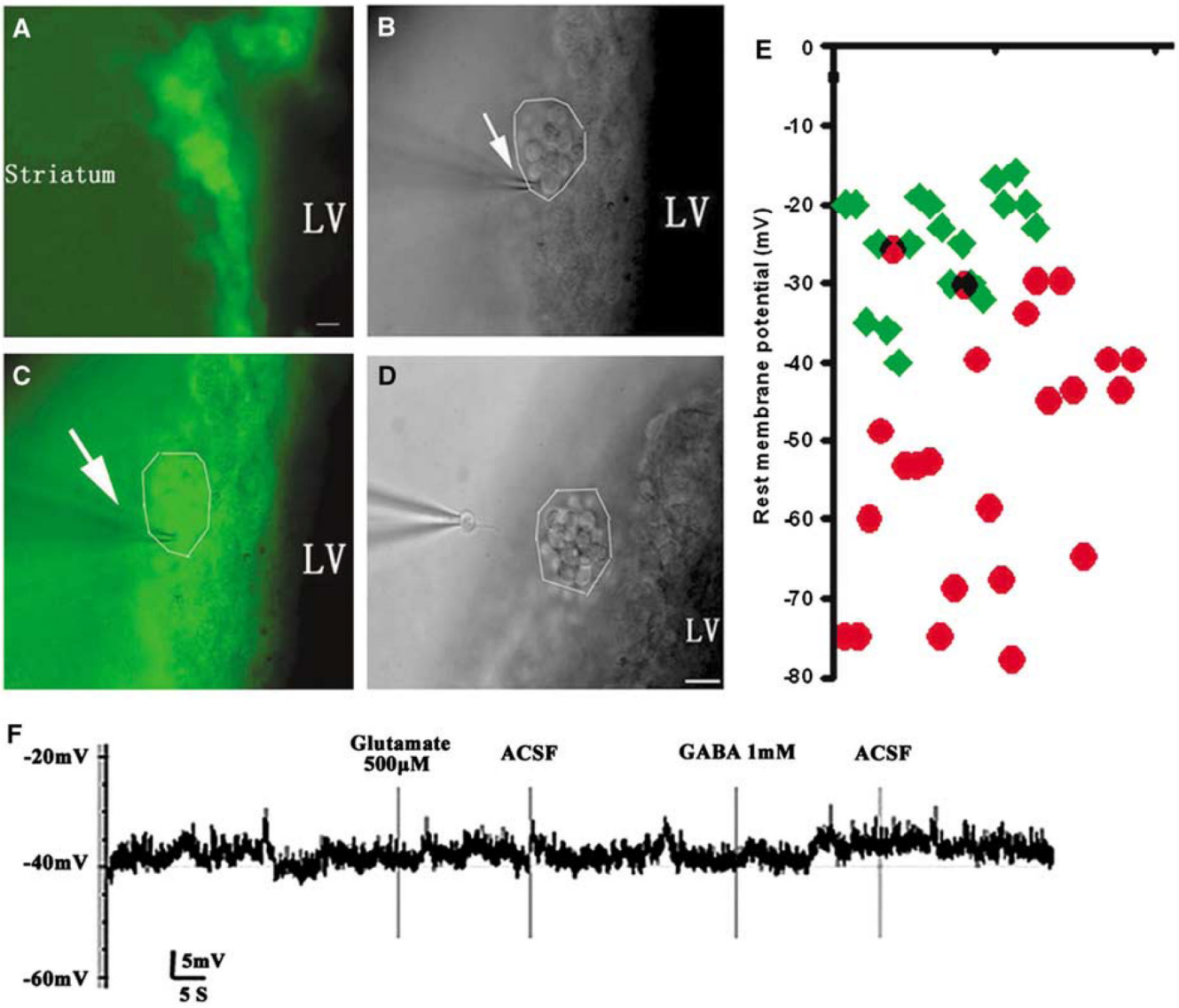

Figure 3.

Electrophysiology of DCX–EGFP-positive cells in the SVZ of the transgenic mouse. Microphotographs show DCX–EGFP-positive cells (green cells) in the SVZ of the lateral ventricle (**A**, **C**). A single DCX–EGFP-positive cell was clamped by the patch clamp from a cluster of DCX–EGFP cells in the SVZ (**B**, **C**). LV indicates lateral ventricle (bar=20 μm). The arrows in (**B**) and (**C**) indicate that the electrode was approaching the DCX–EGFP-positive cells. After patch clamp, the single cell was captured (**D**). The scatter plots of RMP of individual DCX–EGFP-positive cells from the ipsilateral (red circle, $n = 30$) and the contralateral (green diamond, $n = 21$), SVZ show that DCX–EGFP cells in the ipsilateral SVZ have a lower average RMP (**E**). DCX–EGFP cells in the contralateral SVZ did not respond to the bath application of glutamate (500 μmol/L, 20 secs) and GABA (1 mmol/L, 20 secs) at RMP −40 mV (**F**).

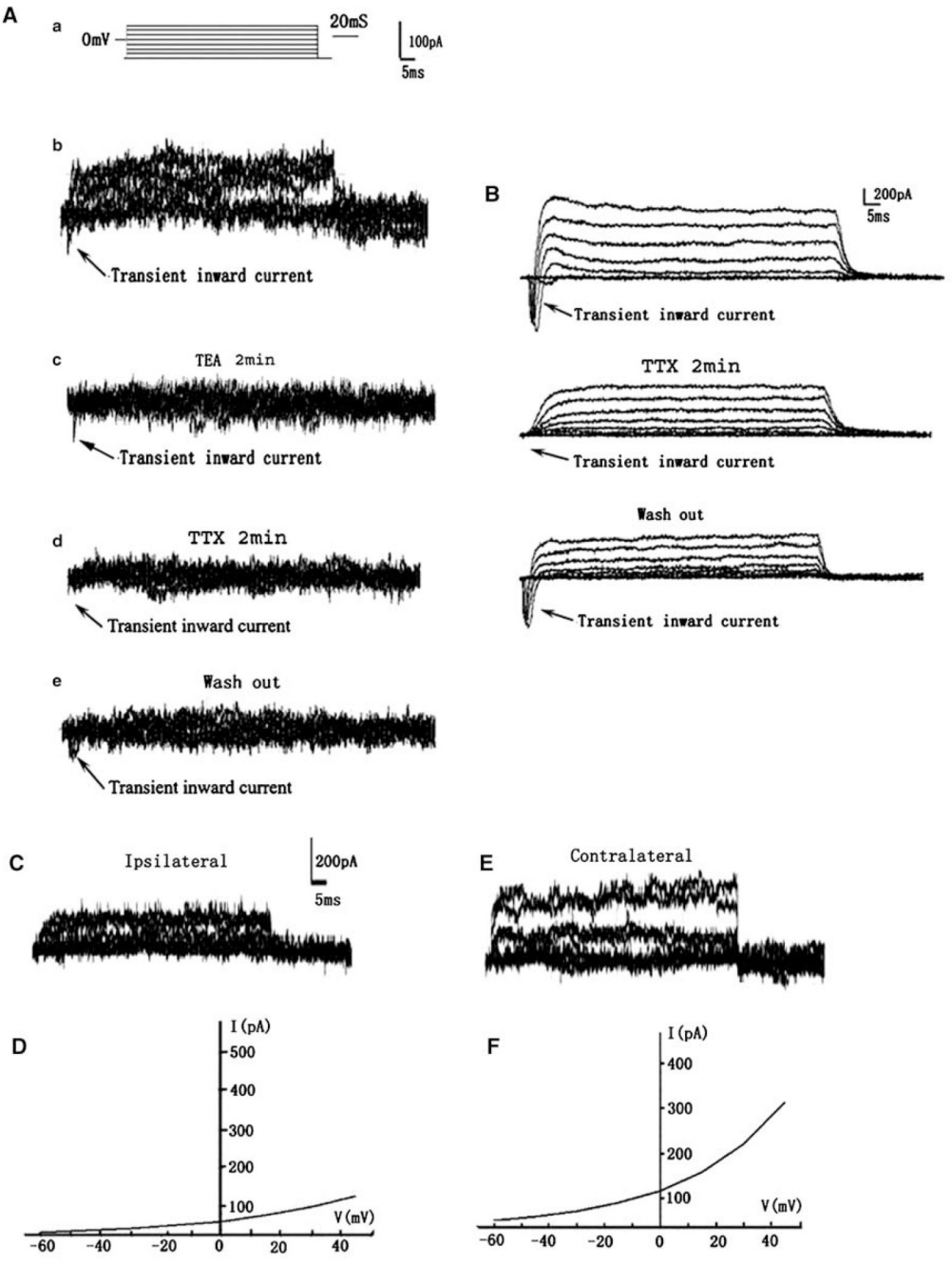

Figure 4.

Sodium and potassium currents from representative DCX–EGFP-positive cells in the ipsilateral or the contralateral SVZ of the adult mice. (**Aa**) The voltage step protocol used in the current study. A lower fast inward current was evoked by voltage steps from −60 to + 45 mV (**Ab**) and a K^+ current inhibitor, TEA (2 mins, 10mmol/L, Ac) blocked K^+ current, but did not inhibit Na^+ current (**Ac**, arrow). However, in the presence of Na^+ current inhibitor TTX (1 μmol/L, 2 mins), the Na^+ current was completely blocked (**Ad**, arrow). At 20 mins after washing out TTX, the current was partially recovered (**Ae**, arrow). (**B**) Typical TTX-sensitive Na^+ currents recorded from nonischemic striatal neuron using the same voltage step protocol. (**C**) A representative DCX–EGFP cell in the ipsilateral SVZ displaying a decrease of whole-

cell potassium current with its *I* to *V* curve (**D**), compared with the current (**E**) and *I* to *V* curve (**F**) of a contralateral SVZ cell.

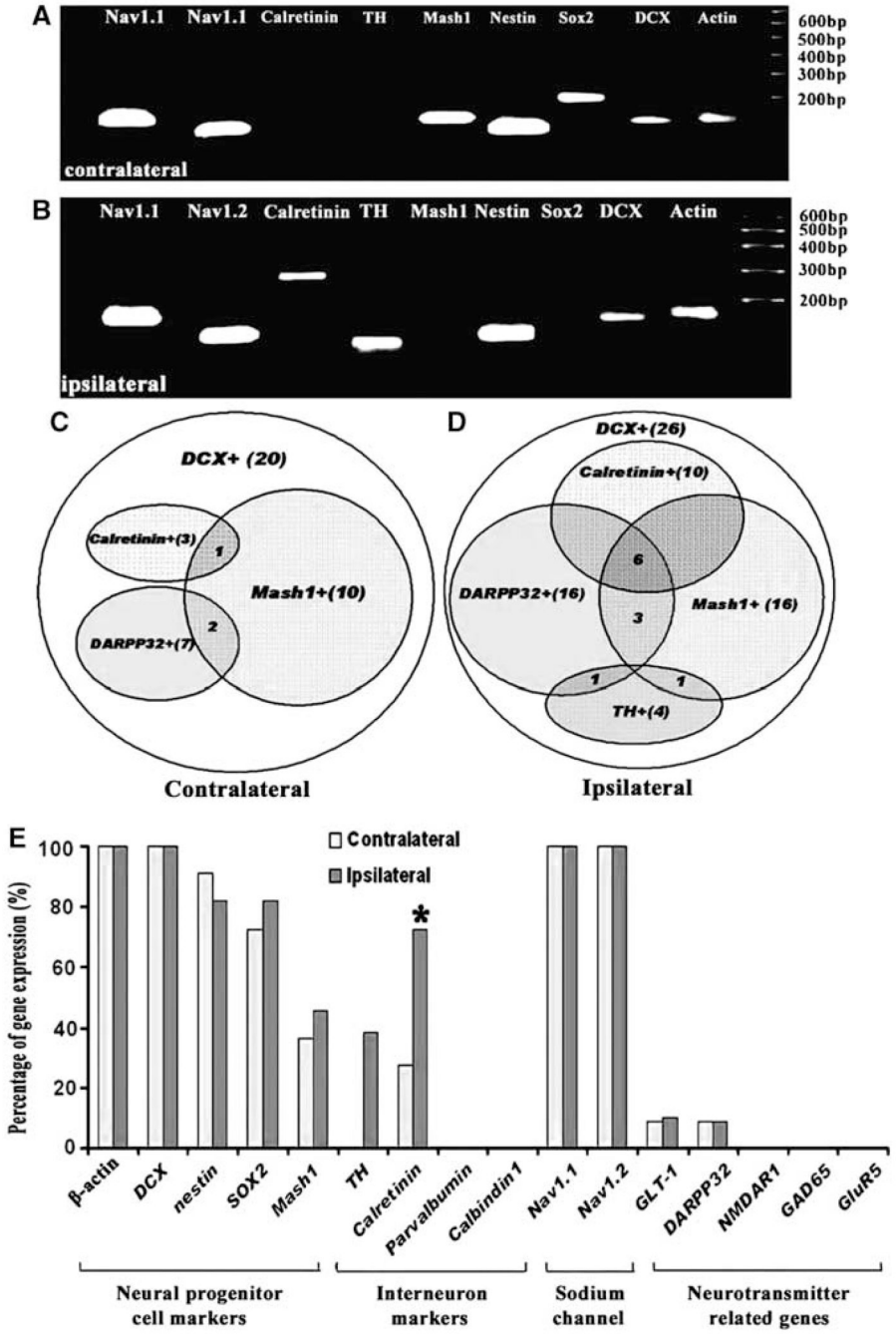

Figure 5.

Gene profiles of a single DCX–EGFP-positive cell in the SVZ of the adult mouse. (**A**, **B**) Single SVZ cell PCR products showing simultaneous expression of nine genes in the contralateral (**A**, *n*=21) or ipsilateral (**B**, *n*=26) DCX–EGFP-positive cell. Note, calretinin and TH genes were expressed in the ipsilateral DCX–EGFP-positive cell (**B**). (**A**) and (**B**) did not include genes that were not detected in both single cells, but they are listed in Table 1. Venn diagrams show the DCX–EGFP cells that coexpressed calretinin, TH, DARPP32, and Mash1 genes in the contralateral (**C**) and ipsilateral (**D**) SVZ. Numbers in (**C** and **D**) indicate cell numbers. (**E**) Frequency of 16 genes examined in the present study. Blue and orange bars represent DCX–EGFP cells in the contralateral and ipsilateral SVZ, respectively. **P* < 0.05.

Table 1

Primers used for detecting genes in a single SVZ cell

Genes	GeneBank accession no.	Primers (from 5′ to 3′)	Sequences	Fragment size (bp)
Primers used in a single cell of the rat				
β-Actin	NM_031144	Sense	CCATCATGAAGTGTGACGTTG	150
		Antisense	CAATGATCTTGATCTTCATGGTG	
DCX	NM_053379	Sense	TTGGACATTTTGACGAACGA	353
		Antisense	CCCTTCTTCCAGTTCATCCA	
GAD65	M72422	Sense	GTTTGATCCGATCCAGGAGA	657
		Antisense	GAGATGACCATCCGGAAGAA	
GFAP	NM_010277	Sense	TAAGCTAGCCCTGGACATCG	110
		Antisense	TTTCTCGGATCTGGAGGTTG	
GluR5	M83560	Sense	CACATTCAGACTCGCTGGAA	487
		Antisense	ATGACACGTGAGGGTTGTCA	
NMDAR1	U11418	Sense	AAGAATGTGACGGCTCTGCT	848
		Antisense	CTGGGTCACCATTGACTGTG	
GLT-1	NM_017215	Sense	GCCAATACAACCAAGGCAGT	280
		Antisense	CACAGATCAAGCAGGCGATA	
Sox2	NM_001109181	Sense	ACCAGCTCGCAGACCTACAT	154
		Antisense	TAGGAGTGGGAGGAAGAGGTA	
Primers used in a single DCX-EGFP cell of the transgenic mouse				
β -Actin	NM_007393	Sense	CCATCATGAAGTGTGACGTTG	150
		Antisense	CAATGATCTTGATCTTCATGGTG	
Calretinin	NM_007586	Sense	CCAGTTCCTGGAAATCTGGA	293
		Antisense	GCCAAGCCTCCATAAACTCA	
Calbindin1	NM_009788	Sense	ATCCCACCTGCAGTCATCTCT	300
		Antisense	AATTCCTCGCAGGACTTCAG	
DARPP32	NM_144828	Sense	CACCCTCCTTTGTACCCTGT	130
		Antisense	AAGAATGACTGGCAGGGAAA	
DCX	NM_001110223	Sense	GAGTGCGCTACATTTATACCATTG	129
		Antisense	TGACATTCTTGGTGTACTCAACCT	
GAD65	L16980	Sense	CGATTTCCATTACCCCAATG	356
		Antisense	GCATGGCATACATGTTGGAG	
GluR5	U31444	Sense	AGCTCTCATGCAGCAAGGAT	224
		Antisense	TCATTGTCGAGCCATCTCTG	
Mash1	NM_022384	Sense	TCTCCTGGGAATGGACTTTG	100
		Antisense	GGTTGGCTGTCTGGTTTGTT	
Nav1.1	NM_018733	Sense	TGTACCACCAGGACCTGACA	129
		Antisense	GGGCCATTTTCATCATCATC	
Nav1.2	NM_001099298	Sense	GAACAACGCATTGCAGAAGA	112
		Antisense	GAAGGGATTTTCCTGCTTCC	
Nestin	BC062893	Sense	GGACAGGACCAAGAGGAACA	107
		Antisense	TCTGGATCCACCTTTTCTGG	

Genes	GeneBank accession no.	Primers (from 5′ to 3′)	Sequences	Fragment size (bp)
NMDAR1	BC039157	Sense	TCTACAGAATCCCCGTCCTG	286
		Antisense	AGCAGAGCCGTCACATTCTT	
Parvalbumin	NM_011393	Sense	GCGGATGATGTGAAGAAGGT	224
		Antisense	GTCAGCGCCACTTAGCTTTC	
GLT-1	NM_011393	Sense	GGCAATCCCAAACTCAAGAA	480
		Antisense	GTCCTTGATGGCGATGATCT	
Sox2	NM_011443	Sense	AGAACCCCAAGATGCACAAC	204
		Antisense	CTCCGGGAAGCGTGTACT TA	
TH	NM_009377	Sense	GAAGGGCCTCTATGCTACCC	354
		Antisense	CCCAGAGATGCAAGTCCAAT	

DARPP32, dopamine- and cAMP-regulated phosphoprotein with molecular weight of 32 kDa; DCX, doublecortin; GAD65, glutamate decarboxylase isoform 65; GFAP, glial fibrillary acidic protein; GLT-1,glutamate transporter 1; NMDAR1, *N*-methyl-D-aspartate receptor 1; TH, tyrosine hydroxylase.

Table 2

Membrane properties of DCX-EGFP cells in the SVZ of the mouse

Groups	C_m (pF)	R_m (mV)	R_a (M)	τ (ms)	Hold (pA)
Non-MCAo (n = 15)	7.1 ± 1.8	201 ± 170	3.7 ± 1.6	22.6 ± 5.1	91.7 ± 14.4
MCAo (n = 16)	7.6 ± 2.4	423 ± 291	2.0 ± 0.8	15.6 ± 1.8*	105.0 ± 44.9

MCAo, middle cerebral artery occlusion.

*$P < 0.05$.